Understanding Complex Adhesive Behaviour: Case Study U-type Bonding Geometry

Anneliese Hagl
A. Hagl Ingenieurgesellschaft mbH, Munich, Germany, a.hagl-ingenieure@t-online.de

In 2000, the Herz-Jesu church was finalized featuring a glass façade with advanced bonded load carrying structures. The façade was stiffened by glass beam elements of lengths up to 6.72 m joined to stainless steel channels by Silicone adhesives. This design required comprehensive experimental and theoretical investigations as conventional guidelines – such as the European guideline ETAG 002 for bonded glass façades – were not applicable. The hereby raised technological questions initiated intensive research investigations in Germany. The failure mechanisms and load carrying capacities of a number of different PFC (parallel flange channels) sections were investigated. The impact of front and side regions on the failure mechanisms was analyzed investigating degraded bonding. This paper presents an overview of the results and gives an outlook on a potential design guideline.

Keywords: Adhesive, Glass Façade, Silicone, Structural Glazing

The Origin: Glass Façade of the Herz-Jesu Church

Design of the Herz-Jesu Church, Munich

The outer structure of the Lord's house Herz-Jesu Church, Munich (commissioned by Erzdiözese München und Freising, Erzbischöfliches Baureferat) has the timeless shape of a rectangular parallelepiped and is built almost completely with glass (Figure 1). The innovative application of glass in the façade serves to emphasize the fundamental idea of the architecture using the style of a rock crystal. Therefore, the architects asked for a glass façade with a minimum of visible load-carrying structures. In order to meet these requirements, two sophisticated structures have been applied. First, horizontally and vertically arranged glass beams serve as supporting – and thus load-carrying – members for the glass façade. Second, the conventional approach extensively using point supports was abandoned in favor of load-carrying line type bonding using Silicone adhesives [1,2].

The skeleton of the glass façade consists of a steel framework stretching out the box shape of the building with the dimensions 47.04 m (length), 19.00 m (width) and 16.00 m (height). The steel framework is based on a of 6.72 m by 6.39 m grid. The primary load-bearing members of the steel framework are eight bending resistant portal steel frames arranged in longitudinal direction according to the raster units (Figure 2). In order to realize load-bearing structures with minimum visibility, the design philosophy of a hanging system has been selected for the glass façade in order to achieve slender frame elements by avoiding destabilizing compression loads. The glass façade consists of the following major components (Figure 3):

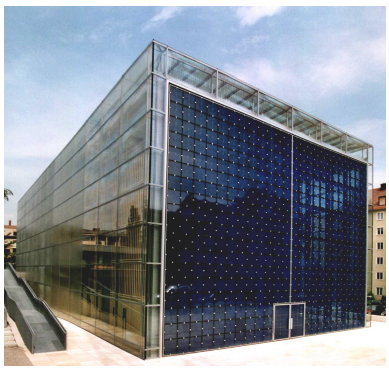

Figure 1: The Herz-Jesu Church, Munich, Germany

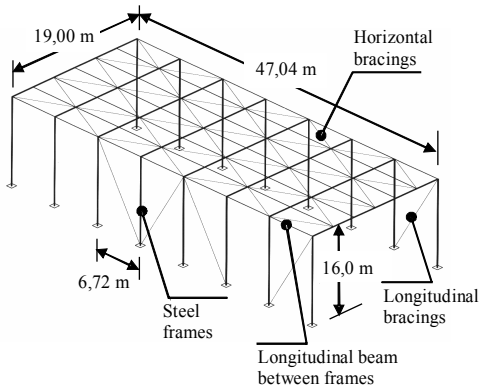

Figure 2: Structural system of the Herz-Jesu Church

- Insulating glass units (width 3.35 m) as core components of the glass façade grouped by two elements within one grid unit
- Horizontal glass beams (length 6.72 m) connecting façade and suspender bars with the steel frames
- Vertical glass beams of varying length fixed to the suspender bars for support of the horizontal glass beams
- Vertically arranged suspender bars directly transferring the dead loads of the insulating glass units, vertical glass beams and façade stringers
- Horizontally arranged façade stringers for wind loading transfer from the insulating glass units to the horizontal glass beams

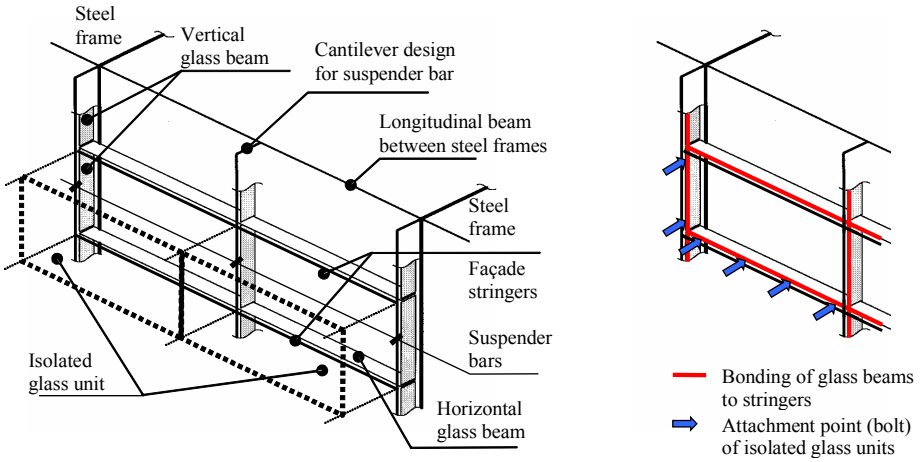

Figure 3: Detail of the hanging system of the glass façade

Bonding of the Glass Beam Elements

For the load-bearing connection of both the horizontal and the vertical glass beams to the suspender bars, the beams were bonded using a Silicone based conventional structural glazing adhesive (DOW CORNING® DC-993) to steel stringers. The steel

stringers are provided with discrete attachment points for connection by bolts to the façade stringers and suspender bars in order to allow easy assembling and maintenance.

The horizontal glass beams have the primary function to transfer wind pressure and wind suction loads acting on the glass façade to the steel frames. In order to establish the load path between glass façade and steel frames, each stringer bonded to a horizontal glass beam has eight attachment points for connection to the horizontal façade stringers. The vertical glass beam supports the horizontal glass beams in order to guarantee the integrity of the structure of the glass façade. The vertical glass beams act like mounting brackets using two fixing points of the bonded stringers for connection to the suspender bars (Figure 4). For generating a reacting moment of the offset of dead loads, a force couple acts on the two attachment points; one loaded by compression, the other – critical one – by tension.

A new philosophy has been applied for the layout of the adhesive joint for preserving the integrity of the bonding and of the glass façade. The special idea consisted in encapsulating the structural adhesive by appropriate selection of steel cross sections in order to tailor the joint regarding structural properties and to protect the adhesive against environmental influences. A channel type section was first choice leading to a three-sided bonding design of U-type, see Figure 4. It is explicitly stated here that this bonding design is not covered by the European guideline ETAG 002 [3, 4] related to structural glazing asking for additional procedures for certification.

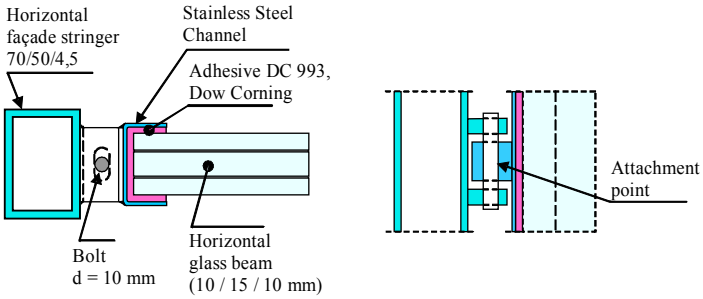

Figure 4: Bonding design glass façade Herz-Jesu Church: Adhesive coloured

Testing of Bonded Glass Beam Elements

Due to the channel sections bonding on one side to the glass beams, these elements show a quite interesting behaviour in case of glass fracture. Compared to conventional laminated glass whose failure mechanism is presented in Figure 5, the broken parts of the glass beams are locked by inner compression still providing limited load-carrying capacities sufficient until repair of the failed component, see Figure 6.

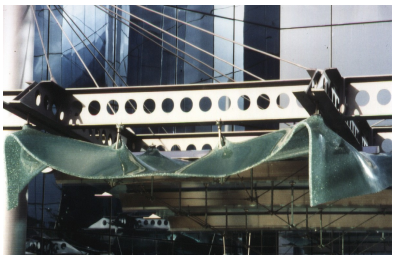

Figure 5: Conventional failure mechanism of tempered laminated glass

Figure 6: Load test of horizontal glass beam element, all glass sheets broken

Furthermore specimens of the envisaged design with 50 mm width were tested in order to substantiate the design of the bonding (Figure 7). The samples were loaded by tension according to the critical load cases encountered by the bonding in the glass façade. Figure 8 shows the mechanical behavior of a sample under a prescribed deformation velocity of 5 mm/min. At a deflection of about 2 mm, the stiffness of the sample decreases significantly although the load-carrying maximum is still not reached. Between deflections of 2 mm and 8 mm, the local stiffness is almost constant. Beyond a deflection of 8 mm, total failure of the specimen occurs after almost doubling the deflection of maximum load demonstrating a behaviour of good nature. For comprehensive understanding of this behaviour, further detailed studies incorporating Finite Element Analysis of the bonding were launched and presented in the next chapter.

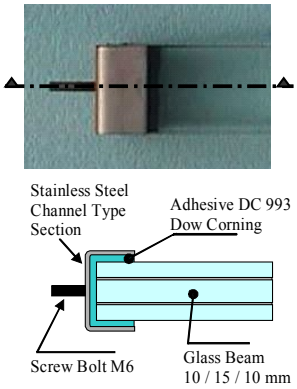

Figure 7: Specimen, Herz-Jesu Church

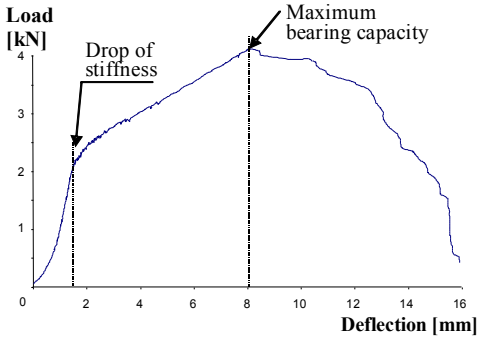

Figure 8: Tension test results of specimen

Modelling of Silicone Adhesives for Bonding Analysis Purposes

Silicone adhesives differ significantly from other adhesives or materials used in civil engineering due to their almost perfect incompressibility and their capability of large

elastic deformations. These properties lead to the classification of Silicone adhesives into the group of elastomeric materials. Elastomerics behave quite different depending on whether they are subject to volume or shape changes. They show low resistance against shape changes such as shear deformations while high stiffness is achieved for volume changes e.g. in the case of hydrostatic pressure loads. For loading under mono-axial tension the material can be extended by multiples of its initial length before rupture. The quasi-static load-deflection curve for tension tests typically starts with a degressive shape as shown in Figure 9 while shear tests often show almost perfect linearity as sketched in Figure 10. Even in the case of high deformations, the material behaves almost perfectly elastic while unloaded. In addition, elastomerics show also time and load-path dependent effects such as visco-elasticity and the Mullins effect, both being beyond the scope of this paper.

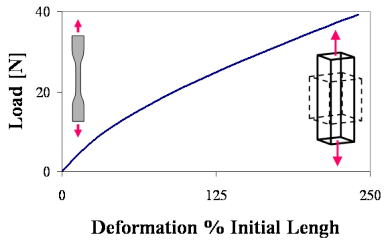

Figure 9: Typical elastomeric (Silicone) behaviour under tension loads

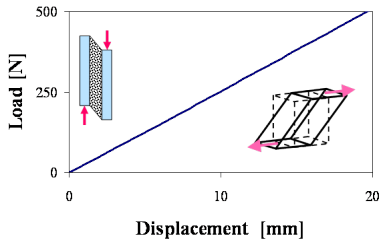

Figure 10: Typical elastomeric behaviour under shear loads

For representation of the elastic behaviour of elastomerics, hyperelastic models are generally available in commercial Finite Element programmes. Hyperelastic material laws are based on an elastic energy potential related to strain energy functions [5,6,7]. The strain energy density W is used to derive stress values σ_{ij} by differentiating with corresponding strain terms ε_{ij} according to the following equation:

$$\sigma_{ij} = \frac{\partial W}{\partial \varepsilon_{ij}} \tag{1}$$

Polynomial laws – Mooney-Rivlin as the most popular – are based on the invariants I1, I2 and I3 of the deformation tensor. For perfect incompressibility (I_3=1), a polynomial approach leads to the following strain energy function:

$$W = \sum_{i+j=1}^{N} c_{ij} (I_1 - 3)^i (I_2 - 3)^j \tag{2}$$

This series approach allows to model arbitrary material behaviour by adequate selection of the coefficients c_{ij}. Dedicated material tests are required for the determination of the coefficients such as mono-axial tension and compression tests, bi-axial tension tests, shear tests and compression tests. For these investigations, mono-axial tension tests as well as shear tests, shown in Figure 9 and Figure 10, were used for calibration of the material law. Values to describe the compressibility of Silicone are taken in accordance to [8].

Review of Experimental Results of Bonding Specimen

For understanding the phenomena leading to the significant drop of stiffness at approximately 2 mm deflection, a Finite Element analysis was performed with focus on the behaviour of the adhesive material. The Finite Element model is presented in Figure 11 showing the adhesive elements in colour. The non-coloured elements represent the PFC section, while the glass body is assumed to be rigid and thus considered only by boundary conditions. A circular rigid body element is used in the centre to load the channel representing the attached screw for load input. The model of the full specimen is shown in Figure 11 for completeness while only a quarter of the model is in fact used for analysis exploiting double symmetry conditions.

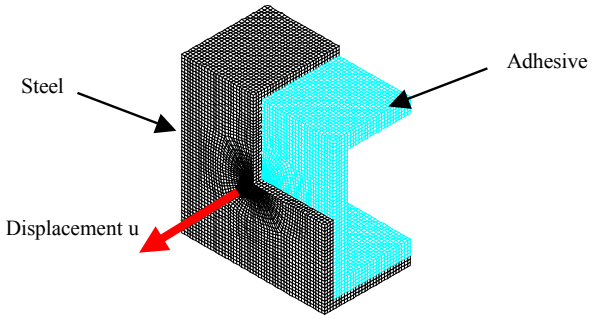

Figure 11: Finite Element Model of the Specimen

Figures 12 and 13 illustrates the stress distribution of this quarter at a load level corresponding to the 2 mm deflection of the specimen test. High loading in terms of high stress levels is visible in the front region of the bonding geometry. A detailed investigation of the numerical results leads to a load distribution of approximately 90% for the tension stresses of the front region and approximately 10% for the shear stresses of the side regions.

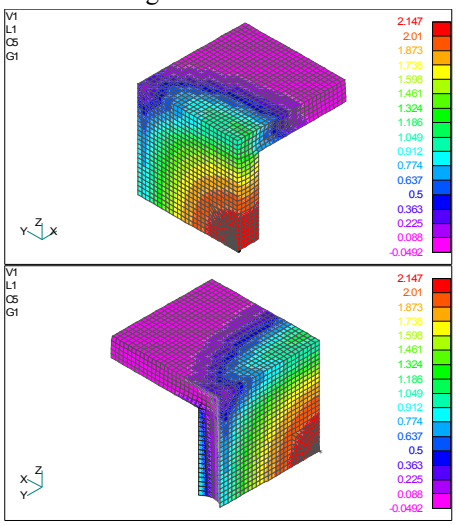

Figure 12: Maximum principal stress distribution (top right quarter)

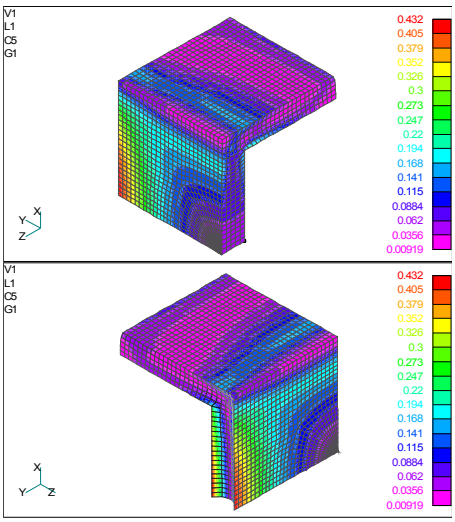

Figure 13: Maximum shear stress distribution (top right quarter)

This load distribution is explained by the high level of incompressibility of the Silicone adhesive. If lateral contraction is not considered while applying simple engineering formula (constant tension stress in the front region, constant shear stress in the side regions), only 60% of the total tension load would be transferred by the front region. For this case the load F obtained by a displacement u – see Figure 11 – is shared between front region (index front) and side regions (index side) according to the following formula for the case of free lateral contraction (E Young modulus, G shear modulus, A reference area, t thickness)

$$F = F_{front} + F_{side} = \left(\frac{EA_{front}}{t_{front}} + \frac{2GA_{side}}{t_{side}} \right) u \tag{3}$$

This load rearrangement is evoked by the dramatically increased stiffness of the front region by preventing the lateral contraction of the adhesive due to the three-sided design and its encapsulating capabilities see also eqs. (4) and (5) taking into account the Poisson ratio ν. The stiffening effect obtained by suppressing lateral contraction is also illustrated in Figure 14, which shows the stiffness ratio with and without lateral contraction. For a Poisson ratio of ν = 0.495, an increase of stiffness by more than factor 30 is obtained. As the suppression of lateral contraction is not perfect for the specimen due to free surfaces, the stiffness increase for the specimen is expected to be lower.

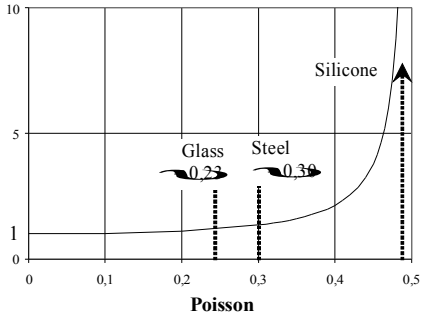

Tension stiffness ratio:

$$\frac{\textit{Tension Stiffness}_{\textit{no lateral contraction}}}{\textit{Tension Stiffness}_{\textit{free lateral contraction}}} = \left(\frac{1}{1+\nu} + \frac{\nu}{(1+\nu)(1-2\nu)} \right)$$

Figure 14: Stiffness ratio free lateral contraction versus suppressed lateral contraction

$$F = \left(\frac{EA_{front}}{t_{front}} \left(\frac{1}{1+\nu} + \frac{\nu}{(1+\nu)(1-2\nu)} \right) + \frac{2GA_{side}}{t_{side}} \right) u \tag{4}$$

Please note that if a perfectly incompressible material (Poisson's ratio υ=0.5) is totally encapsulated by rigid boundaries, tension or compression stiffness is infinite:

$$\frac{EA_{front}}{t_{front}} \left(\frac{1}{1+\nu} + \frac{\nu}{(1+\nu)(1-2\nu)} \right) \to \infty \quad \text{for } \nu \to 0.5 \tag{5}$$

These graduated stiffness and loading properties of front and side regions have lead to the following hypothesis concerning fracture mechanics [1]. If the bonding is

overloaded, the front region will partially or totally fail due to the high stresses under the related operating conditions. In this case, the stiffness of the entire bonding will drop as the damaged front region results in increased flexibility. In case of the load is still beeing present, the side regions whose load carrying capabilities are not damaged will establish the load transfer in a more flexible manner. The deflection at maximum load (approximately 8 mm) confirms this hypothesis as the related maximum shear strain corresponds to those experienced with ETAG specimen. In order to validate this hypothesis new investigations were launched analyzing different kind of bonding degradations [9, 10].

Investigation of Degraded U-type Bonding Geometries

Looking into more details in the behaviour of U-type bonding geometries, first indication to confirm the above mentioned hypothesis is found in Figure 15 showing a specimen test of another U-type bonding [11]. The picture series demonstrates clearly that the failure of the material is indeed initiated in the front region of the bonding geometry confirming that the high loading in this area is critical with respect to bonding integrity. The next step comprising both experimental and numerical activities consisted in the analysis of U-type bonding assemblies in a systematic manner with front or side regions disabled, see Figure 16. The related regions were disabled by inserting PE-layers before application of the adhesive. Table 1 presents some key results of the related experimental results – this time performed with Aluminum channels loaded edgewise:

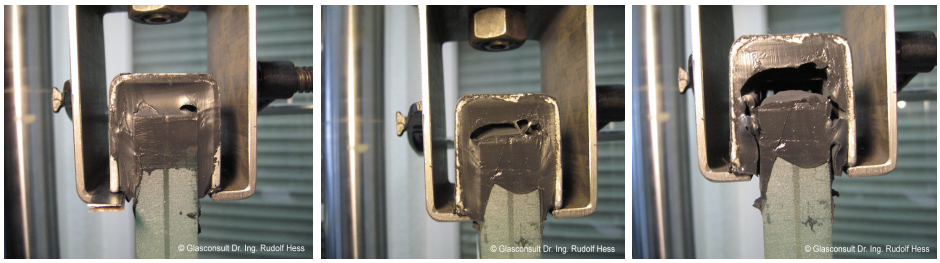

Figure 15a, b and c: Testing of U-type bonding

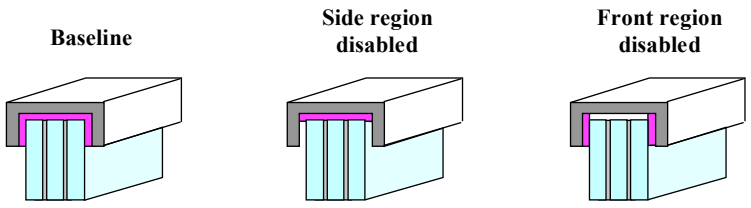

Figure 16a, b and c: Bonding configurations

The overall behaviour of the experimental results for different configurations is shown in Figure 17. In this figure, the correspondence of baseline and side-region-disabled configurations for displacements larger than 10 mm demonstrates that for these high deformations load is transfered mainly by the side region as it was hypothesized in the chapter before. In Figure 18 numerical results are presented for the three different configurations. In coincidence with table 1 high stiffness is obtained for all configurations with operative front region i.e. baseline and side region disabled while

very low stiffness is observed for operative side regions only i.e. front region disabled. Furthermore, the stiffness levels for the latter case of operative side regions only are quite similar for experimental and numerical results whereas the level of coincidence for the cases with operative front side is lower. It is assumed that this behaviour is due to unmodelled flexibilities of the experimental test set-up showing a larger impact on stiff specimen.

Table 1: Key numbers of U-type bonding with and without degradation

Bonding status	Initial specimen stiffness [N/mm]	Beginning fracture Load [N]	Beginning fracture Displacement [mm]	Maximum load Load [N]	Maximum load Displacement [mm]
Perfect bonding	2080	3400	2.6	4500	8.2
Side regions disabled	795	3000	4.6	3200	6.5
Front region disabled	310	n/a	n/a	2600	14.1

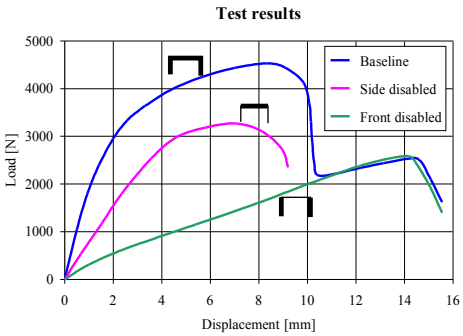

Figure 17: Experimental results for different bonding configurations (averaged over specimens)

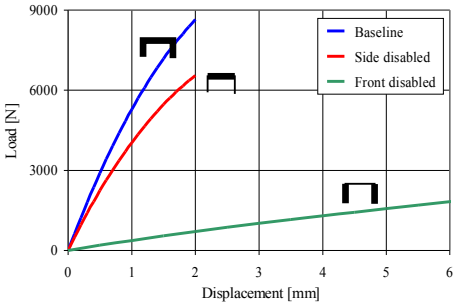

Figure 18: Numerical results for different bonding configurations

Figure 19 compares stress distributions for the various configurations. As the loading in the numerical analysis is controlled by prescribed deformations of the channel section, a deflection of the channel was selected related to maximum load carrying capacities with fully operative front region. For these configurations, the maximum principal stress levels are comparable and amounts to approximately 2.1 N/mm^2. If only the side region is enabled, the specimen behaves like a simple shear specimen showing high flexibility. The behaviour shown in Figure 19 can be found by very low stress levels although the prescribed deformation is in the same magnitude. For bonding designs of type shear only, it is obviously adequate to use experimental limit values of the related material shear tests. Concluding these results the U-type bonding typically starts to fail in the front region area due to high stress levels showing a significant stiffness reduction. If load still increases, the additional loads will be transferred to the side regions resulting in a lower effective overall stiffness.

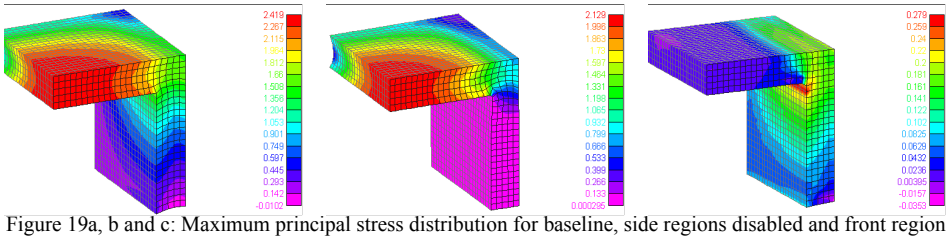

Figure 19a, b and c: Maximum principal stress distribution for baseline, side regions disabled and front region disabled

Parameter Variations of U-type Bonding Geometries

The design of a U-type bonding geometry is characterized by the following three parameters:

- Adhesive thickness of the front and side regions
- Front region area defined by the thickness of the glass body
- Side region area defined by the size of the U-type channel cross section

An adequate choice of adhesive thickness is typically given by the adhesive manufacturers based on experience of processing this kind of material. According to today's knowledge, an adhesive thickness between 5 mm and 12 mm is state of the art for Silicones used in structural glazing. Typicall glass elements are designed for load requirements this means that width parameters of the U-type channel cross section has to be chosen appropriately. Furthermore, the front region is also defined by the thickness of the glass elements. Regarding the side region, the related area is determined by adequate choice of the selected cross selection of the U-type steel elements.

Based on the experience of the last chapter the following impacts of geometry on load-carrying capacity are expected: - First an increase of the front area should lead to higher loads before drop of stiffness due to the beginning of the failure of the front region means that the glass thickness also defines this particular point. - Second, an increase of the side area should strengthen the secondary load path via shear loads meaning that an increase leads to an improvement of the load behaviour after partial or total failure in the front region. Consequently, the overall failure of the bonding can be designed with this geometry parameter.

In order to validate these statements by experimental results, tests were performed for a bonding geometry with reduced side areas according to geometry data in Figure 20. Table 2 presents key results of the related tension tests.

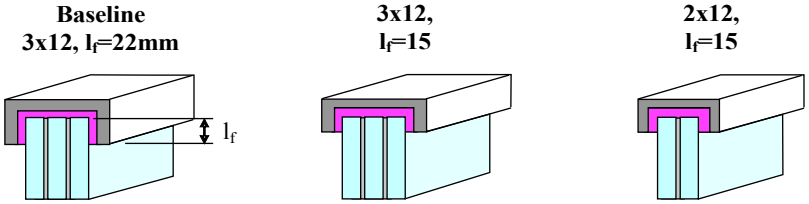

Figure 20a, b and c: Investigated bonding geometries

Table 2: Key numbers of U-type bonding of different geometry

Bonding status	Initial specimen stiffness [N/mm]	Beginning fracture Load [N]	Beginning fracture Displacement [mm]	Maximum load Load [N]	Maximum load Displacement [mm]
Baseline 3x12 l_f=22mm	2080	3400	2.6	4500	8.2
3x12 l_f = 15 mm	1530	3200	3.0	3650	5.1
2x12 l_f = 15 mm	760	3100	2.2	3400	2.7

Figure 21 shows a comparison of the general behaviour for different configurations. Figure 22 compares the stress levels obtained for a load level corresponding to the experimentally detected drop of stiffness for the cases with modified side and front area.

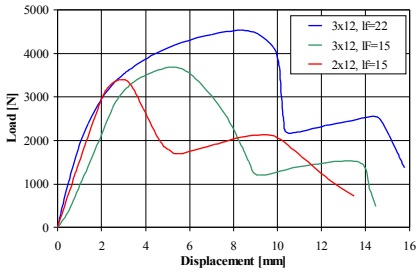

Figure 21: Experimental results for different bonding geometries (averaged over specimens)

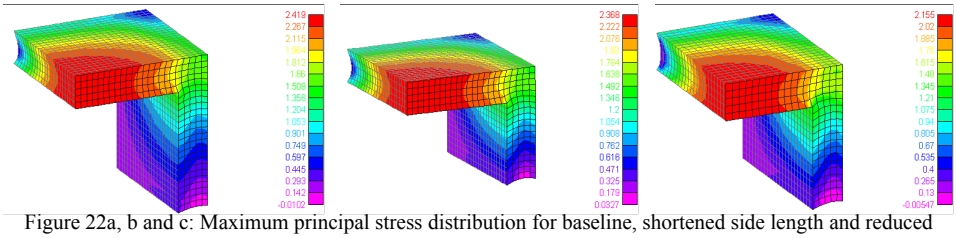

Figure 22a, b and c: Maximum principal stress distribution for baseline, shortened side length and reduced glass thickness

The significant role of the front region regarding high stress levels and related stiffness is clearly visible here. Therefore, the following conclusions can be drawn:

- For a perfect U-type bonding, the contribution of the side region to initial stiffness and load-carrying capacity is limited compared to the front region.
- The load-carrying capacity is mainly given by the front region and thus indirectly by the thickness of the glass body. Nevertheless, the differences in Figure 21 are less than expected.
- After the failure started to occure in the front region the loads will be increasingly transferred to the side regions. This effect allows to design the fracture behaviour after the failure occurred in the front region.

Sizing of U-type Bonding Geometries

Typically, the bonding behaviour is tested using specimens of a certain width, e.g. 50 mm due to hardware requirements such as limited loads by the test apparatus and/or load introduction. It was highlighted in the chapters before that the suppression of the lateral contraction evokes the remarkable behaviour of the U-type bonding while applying an almost incompressible adhesive. This issue automatically leads to the question whether the results obtained by specimens of limited width can be transferred to long bonding geometries as in the case of the glass façade. It should be kept in mind that the level of suppression of lateral contraction is a function of bonding length. On the one hand – in the case of very long bondings, almost perfect plain strain states – characterized by perfect suppression of lateral contraction – can be assumed for the bonding with the exception of the free surface region. On the other hand, plain stress states – characterized by free lateral contraction – can be assumed for very small bonding geometries which are typically not relevant here and in the vicinity of the free surfaces regions. Figure 23 shows different stress distributions for the baseline bonding geometry of varying length. The figure leads to the conclusion that the free surface affects stress distribution in the front region up to the magnitude of the thickness of the U-type channel.

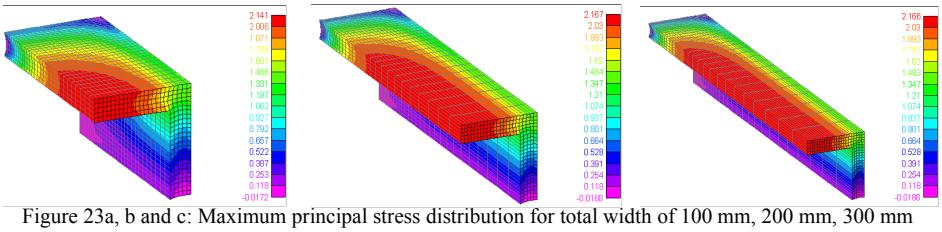

Figure 23a, b and c: Maximum principal stress distribution for total width of 100 mm, 200 mm, 300 mm

This behaviour allows different conclusions. First, experimental load tests using specimens of limited width are assumed to be conservative in the sense that the stress distribution shows higher non-uniformity due to larger free surface effects. Subsequently – the load-carrying capacities are expected to be smaller as high stress peaks initiating the failure of the front region will occur for lower load levels. Second, the assumption of pure plain strain states for the entire bonding is estimated to be non-conservative as the free surface effects leads to higher loading of the undisturbed regions. Third, the assumption of plain stress states is generally not adequate for this kind of application. Analysing the loaded bonding more in depth, Figure 24 and Figure 25 present the load transfer for a given displacement for varying bonding length emphasizing the free surface effect for low width by low transferred loads and the stiffening effect of suppressing lateral contraction inside the bonding for increased widths. For lengths larger than 50 mm, a plain strain sate can be assumed inside of the assembly. In contrast, the outer 50 mm of the bonding are affected by free surface effects leading to complex 3D states. A rough estimation of the load-carrying capacities can be made by neglecting the outboard region in case of knowledge of the limit loads for plain strain states. Assuming that the presented curves refer to the maximum load levels for a fully operative front region, the figure can directly be used for designing the width of a bonded member with the same cross section.

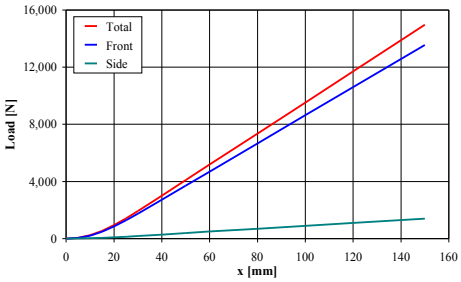

Figure 24: Load transfer of baseline U-type bonding for varying width

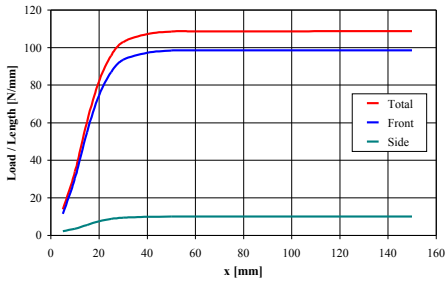

Figure 25: Distributed loads for baseline U-type bonding for varying width

Table 3 presents the related loads assuming plain stress and plain strain states for the analysed bonding geometry. This table underlines the necessity which takes the suppression of lateral contraction leading to high stiffness into account and thus to high loads in the front region. The side regions remain "soft" due to deformations dominated by shear and not affected by incompressibility issues. This behaviour is highly appreciated as thermal loads evoked by different thermal coefficients of glass, adhesive and channel material might lead to significant thermal stresses for bonding geometries with large width such as in the case of the Herz-Jesu Church the glass beam elements with 6.72 m maximum length.

Table 3: Load transfer shares assuming plain stress and plain strain states for baseline geometry

Baseline geometry	Plain stress state	Plain strain state
Total	9.9 N/mm	108.7 N/mm
Front region	7.6 N/mm	98.5 N/mm
Side regions	2.3 N/mm	10.2 N/mm

Conclusions

For the glass façade of the Herz-Jesu Church, Munich, extensive use was made of load-carrying bonding using Silicone adhesives. The baseline bonding geometry consists of a U-type bonding mainly intended to emphasize the transparency of the glass façade and to reduce visibility of the load-bearing structure. During design and construction, it was noticed that this kind of U-type bonding offers a lot of additional advantages in the fields of:

- Load bearing capacity
  - Redundant load paths by front and side regions of U-type bonding geometry
  - Favourable fracture behaviour by load path shift from front to side regions in case of overloading conditions
- Elasto-mechanic behaviour
  - High joint stiffness for tension due to suppressed lateral contraction of the adhesive material
  - Low joint shear stiffness in longitudinal direction, thus favourable behaviour with respect to thermal loading

- Aging/Durability
    - Protection of highly loaded front side by encapsulating of the adhesive
    - Small and almost unloaded free surface leading to high robustness against environmental impact

In order to generalize the characteristics of this kind of bonding, additional investigations were performed analysing the load transfer and the failure mechanisms in detail. The different influences of the front and side regions of the geometry on the bonding properties were identified in depth by analyzing different configurations (baseline, side regions disabled, front region disabled) and different geometries (varying side regions, different glass thickness). In the following, related design rules were concluded and 3D effects on the free surface were analysed in detail, leading to an estimation of efficiency loss for varying length.

Acknowledgements

The author would like to thank the customer – Erzdiözese München und Freising, Erzbischöfliches Baureferat – for unconditional support of the advanced design of the Herz-Jesu Church, Munich. Furthermore, the author would like to thank the Dow Corning company for their outstanding technical support provided during the design of the façade as well as in the related research phase. The author acknowledges as well the organisations of the "Fachverband Konstruktiver Glasbau" (FKG) and the "Labor fuer Stahl- und Leichtmetallbau" at the Munich University of Applied Sciences providing a platform for research.

References

[1] Hagl, A., *Synthese aus Glas und Stahl: Die Herz-Jesu Kirche, München*, Stahlbau 71 (2002), pp. 498-506.

[2] Hagl, A., *Ästhetisch, kostengünstig, innovativ: Neue Verbindungstechnik für tragende Glasstrukturen*, Deutsches Ingenieurblatt April 2003, pp. 14-21.

[3] ETAG 002 *Guideline for European Technical Approval for Structural Sealant Glazing System (SSGS) - Part 1 Supported and unsupported systems*, www.eota.be/pdf/ssgs-fin-am3.pdf.

[4] Hagl, A.*, Kleben im Glasbau, Stahlbaukalender 2005, Herausgeber Kuhlmann U., Verlag Ernst & Sohn, 2005, pp. 819-861.*

[5] Holzapfel, G.A., *Nonlinear solid mechanics – A continuum approach for engineering*, John Wiley & Sons, Chichester, 2000.

[6] Seibert, D.J., Schöche, N., *Direct comparison of some recent rubber elasticity models*, Rubber Chemistry and Technology Vol.73 2000, pp. .366-384.

[7] Charlton, D.J., Yang, J., Teh, K.K., *A review of methods to characterize elastic behaviour for use in finite element analysis*, Rubber Chemistry and Technology Vol.67 1994, pp. 481-503.

[8] Wolf, A.T., Descamps, P.: *Determination of Poisson's ratio of Silicone sealants from ultrasonic and tensile measurements*, Performance of Exterior Building Walls, ASTM STP 1422, P.G. Johnson, Ed., American Society for Testing and Materials, West Conshohocken, PA, 2002.

[9] Fachhochschule München, FB02, *Geklebte Verbindungen im Konstruktiven Glasbau*, Forschungsbericht, abgeschlossenes BMBF Projekt, AIF-Nr.: 1755X04, 2007.

[10] Hagl, A.*, Klebungen bemessen- Tragende Verklebungen mit Silikon, Tagungsband: Glas im Konstruktiven Ingenieurbau V, 2007, Herausgeber Bucak, Ö., Fachhochschule München.*

[11] Glasconsult, Hess, Dr R., 8142 Uitikon, Swizzerland*, Testing of a U-type-Bonding as safety devicesod the glass panels od various glass soundbarier walls along freeeways in the vincinity od Zürich.*